JOURNAL OF Materials CHEMISTRY

Nickel oxide supported on zirconium-doped mesoporous silica for selective catalytic reduction of NO with NH_3†

Ramón Moreno-Tost, José Santamaría-González, Pedro Maireles-Torres, Enrique Rodríguez-Castellón* and Antonio Jiménez-López

Departamento de Química Inorgánica, Cristalografía y Mineralogía, Facultad de Ciencias, Universidad de Málaga, 29071 Málaga, Spain. E-mail: castellon@uma.es

Received 26th April 2002, Accepted 2nd July 2002
First published as an Advance Article on the web 3rd October 2002

A zirconium-doped mesoporous silica with MCM-41-type structure has been used as a support for nickel oxide and tested in the selective catalytic reduction (SCR) of NO with ammonia. From XPS and H_2-TPR data, two kinds of catalysts can be prepared, depending on the nickel loading. Thus, low nickel loadings (1 and 3 wt%) give rise to small particles located in mesopores, whereas higher nickel contents (6 and 12 wt%) favour the formation of larger nickel oxide particles, mainly situated on the external surface. Moreover, the small particles are less reducible, owing to their strong interaction with the internal surfaces of the support. The catalyst with a nickel loading of 6 wt% is very active in the SCR of NO with NH_3 at 400 °C, leading to an NO conversion of close to 60%, with a selectivity towards N_2 close to 100% and formation of a negligible amount of N_2O. From the experimental data, a correlation between reducibility and catalytic activity can be established.

Introduction

The emission of NO_x gases, produced during high temperature combustion processes, is one of the worst environmental problems caused by man. NO_x is oxidised to nitric acid by oxygen from the atmosphere, contributing to acid rain and, furthermore, the photolysis of NO_2 leads to the formation of ozone. Both processes cause serious damage to flora and fauna. To date, the best way to solve this problem is the selective catalytic reduction (SCR) of NO_x by using different types of catalysts based on noble metals supported on ceramic supports for mobile sources,[1] and vanadium(v) oxide supported on WO_3/TiO_2 using ammonia as the reducing agent for stationary sources.[2] However, due to the high toxicity of vanadium and to the oxidation of SO_2 to SO_3 catalysed by vanadium(v) oxide, other highly active catalysts, such as redox-active phases supported on zeolites, have been studied using NH_3 or hydrocarbons as reducing agents.[3,4] However, the zeolites are not very stable at high temperatures in moist feed, and sometimes their catalytic behaviour is affected by the binder substances used during the manufacturing of the extrusions.[5]

Very recently, a zirconium-doped mesoporous silica, with an Si/Zr molar ratio of 5 (SiZr5), has been successfully tested as support for cobalt oxide[6] and copper oxide[7] in the SCR of NO using ammonia as the reducing agent. This modified mesoporous silica belongs to the well-known family of MCM-41 materials,[8] which present a hexagonal arrangement of cylindrical channels with diameters ranging between 16 and more than 100 Å. Previously, Yang *et al.*[9] investigated the activity of NO in SCR over Fe^{3+} ion-exchanged aluminium-doped mesoporous silica (Al-MCM-41) and obtained NO conversion values near to 40% at 350–450 °C. In the above mentioned cases, MCM-41-type materials doped with heteroatoms such as Al or Zr were selected as supports due to their enhanced acidity, with the aim of improving SCR activity by facilitating the access of the reactant molecules to the active centres by supporting them on a mesoporous support.

Nickel oxide species are not generally used as active phases in the SCR of NO, but, recently, Ma *et al.*[5] reported the preparation of a composite containing Ni-exchanged ZSM-5 supported on Raney-Ni, and they observed remarkable de-NO_x activity when using ammonia as the reducing agent. The observed selectivity was even higher than that observed with a Cu-exchanged ZSM-5/Raney-Ni composite. Highly dispersed NiO on γ-Al_2O_3 also exhibits a high catalytic activity for the SCR of NO using propene as the reducing agent.[10] These antecedents led us to investigate the potential use of nickel oxide supported on mesoporous SiZr5 for NO SCR using ammonia as the reducing agent.

There are relatively few publications in the literature concerning the preparation and application of nickel supported on mesoporous materials.[11–13] The most widely used method to incorporate nickel consists of incipient wetness impregnation with nickel nitrate as the precursor salt.[11–15] Lensveld *et al.*[11] have characterised MCM-41-supported nickel oxide catalysts (10 wt% Ni) prepared by using different nickel precursors and they observed, when nickel nitrate is employed, a bimodal particle size distribution with small nickel oxide particles inside the mesopores and relatively large particles (>100 Å) on the external surface of the support.

In this paper, we present the preparation and characterisation of nickel oxide supported on a zirconium-doped mesoporous silica with different nickel contents (1–12 wt% Ni), and their application in NO SCR using ammonia as the reducing agent, in the presence of an excess of oxygen. The choice of this mesoporous support is due to the fact that the introduction of zirconium into a silica matrix may favour the interaction with active phases based on transition metal oxides. Hence, it is expected that a high metal oxide–support interaction could impede the agglomeration of the metal oxide particles and the subsequent formation of crystallites, thus high dispersion degrees could be reached. In a word, for a given support, although the textural properties important (specific surface area, pore volume and pore size distribution), the type of interaction between the support and a particular active phase is even more so.

Experimental

SiZr5 (Si/Zr molar ratio of 5) was prepared by following the method described in previous papers.[16,17] This support was

†Basis of a presentation given at Materials Discussion No. 5, 22–25 September 2002, Madrid, Spain.

DOI: 10.1039/b204041g

impregnated with different aliquots of a nickel(II) nitrate ethanolic solution (1, 3, 6 and 12 wt% Ni) by using the incipient wetness method. After impregnation, the solvent was evaporated at 60 °C and the solids were then calcined in air at 550 °C for 4 h, with a heating rate of 1 °C min^{-1}. The catalysts are labelled as SiZr5-*X*Ni, where *X* is the weight percentage of nickel.

Elemental chemical analyses were performed by atomic absorption spectroscopy using a Perkin-Elmer 3100 spectrometer. Powder XRD patterns were obtained with a Siemens D500 diffractometer, equipped with a graphite monochromator and using Cu-Kα radiation. X-Ray photoelectron spectra were collected using a Physical Electronics PHI 5700 spectrometer with non-monochromatic Mg-Kα radiation (300 W, 15 kV, 1253.6 eV) and with a multi-channel detector. Spectra of powdered samples were recorded in the constant pass energy mode at 29.35 eV, using a 720 μm diameter analysis area. During data processing of the XPS spectra, binding energy values were referenced to the C 1s peak (284.8 eV) from the adventitious contamination layer. The PHI ACCESS ESCA-V6.0 F software package was used for acquisition and data analysis. A Shirley-type background was subtracted from the signals. Recorded spectra were always fitted using Gauss–Lorentz curves, in order to determine the binding energy of the different element core levels more accurately. The error in BE is estimated to be *ca*. 0.1 eV. Diffuse reflectance UV-VIS-NIR spectroscopy was performed by using a Shimadzu 8100 spectrometer and $BaSO_4$ as the reference. Temperature-programmed reduction with hydrogen (H_2-TPR) was performed as described previously.[18] The specific surface area and pore volume were calculated from the N_2 adsorption–desorption isotherms at −196 °C, obtained in a conventional glass volumetric apparatus. Temperature-programmed desorption of ammonia (NH_3-TPD) was used to determine the total acidity of the catalysts and was carried out as described elsewhere.[17,18]

Temperature-programmed desorption of NO (NO-TPD) was performed by adsorbing NO on the catalysts at room temperature (150 cm^3 min^{-1} flow rate and 0.05 vol% NO balanced with He) for 1 h, and desorption between 40 and 550 °C (heating rate 10 °C min^{-1}). Before the adsorption of NO, the catalysts were heated at 550 °C under an He flow for 1 h. During the desorption, helium was employed as the carrier gas and the composition of the evolved gases was determined by using an on-line Balzer GSB 300 02 quadrupole mass spectrometer.

The four catalysts were tested for NO SCR by using a Pyrex glass tube micro-reactor (0.27 in. o.d.) in a steady-state flow mode. About 150 mg of pelletised solids (0.3–0.4 mm) were set into the reactor and plugged with glass wool. Before the catalytic runs, the catalysts were pretreated at 350 °C *in situ* for 2 h under a helium flow. The reaction mixture consisted of 1000 ppm NO, 1000 ppm NH_3 and 2.5 vol% O_2 (balanced with He). The flows were independently controlled by channel mass flowmeters (Brooks) and a total flow rate of 42 cm^3 min^{-1} was used in the feed. Under these experimental conditions, the space velocity (F/W) was 3300 h^{-1}. The reaction temperature interval explored was 100–600 °C. During the catalytic reaction, NO, N_2O, N_2 and NH_3 concentrations were monitored by using the on-line quadrupole mass spectrometer mentioned above.

Results and discussion

Characterisation of catalysts

Fig. 1 shows the powder X-ray powder diffraction patterns, at low angles, of the catalysts with different nickel loadings. The incorporation of nickel oxide produces a broadening of the d_{100} reflection line, and this broadening progressively increases with increasing nickel loading. At the same time, the d_{100} line is shifted from 44.2 Å for the support (SiZr5) to 34.0 Å for the SiZr5-1.5Ni catalyst (see Table 1). The diffractograms at high angles (Fig. 1) of the catalysts with a higher nickel loading (SiZr5-6Ni and SiZr5-12Ni) show reflection lines at 2.41, 2.09 and 1.48 Å, the intensities of which increase with metal loading, which are the characteristic diffraction lines of NiO. The estimation of the size of the NiO particles present on the SiZr5-12Ni catalyst (from XRD by using the Debye–Scherrer equation) provides a value close to 40 nm. However, the patterns of the catalysts with lower nickel loading do not exhibit NiO reflections. This means that, in the latter case, very small nickel oxide particles are formed, probably located inside the mesopores of the SiZr5 support, thus attaining a good dispersion.

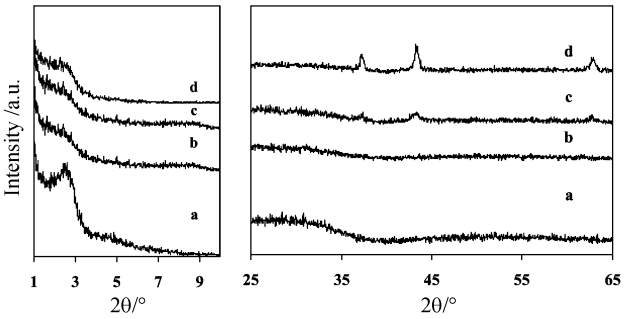

Fig. 1 Powder XRD patterns of SiZr5-1.5Ni (a), SiZr5-3Ni (b), SiZr5-6Ni (c) and SiZr5-12Ni (d) catalysts.

Table 1 Textural parameters and total acidity values for nickel oxide supported on zirconium-doped mesoporus silica catalysts

Catalyst	d_{100}[a]/ Å	S_{BET}/ m^2 g^{-1}	V_p[b]/ cm^3 g^{-1}	d_p[b]/ Å	Total acidity[c]/ μmol NH_3 g^{-1}
SiZr5	44.2	632	0.615	30.9	389
SiZr5-1.5Ni	34	666	0.666	30.4	502
SiZr5-3Ni	—	510	0.470	37.5	627
SiZr5-6Ni	35.9	512	0.351	30.3	526
SiZr5-12Ni	35.9	565	0.564	31	360

[a]Determined by XRD. [b]Accumulated pore volume and average pore diameter calculated using the Cranston–Inkley method. [c]As determined by NH_3-TPD.

The diffuse reflectance electronic spectra of the catalysts with low nickel content (SiZr5-1.5Ni and SiZr5-3Ni) hardly display any absorption bands, whereas the other catalysts give rise to broad and weak bands at 26 400, 13 700 and 9500 cm^{-1} that can be assigned to the $^3T_{1g}(P) \leftarrow {}^3A_{2g}$, $^3T_{1g} \leftarrow {}^3A_{2g}$, and $^3T_{2g} \leftarrow {}^3A_{2g}$ transitions, respectively, and are similar to those observed for NiO/MgO (24 600, 13 500 and 8600 cm^{-1}).[19]

Concerning the Ni/Zr molar ratios on the surface (as determined by XPS) and in the bulk (Table 2), they are very similar for the catalysts with a low nickel content. However, higher nickel loadings (SiZr5-6Ni and SiZr5-12Ni) lead to surface Ni/Zr molar ratio values lower than those observed in the bulk. This fact can be explained by taking into account the large particle size of the NiO deposited on the surface of the support,

Table 2 Binding energies in eV for the Ni $2p_{3/2}$ and Ni $2p_{1/2}$ core levels and surface and bulk Ni/Zr molar ratios, as determined by XPS and chemical analysis, respectively

Catalyst	Ni $2p_{3/2}$/ eV	Ni $2p_{1/2}$/ eV	Surface Ni/Zr molar ratio	Bulk Ni/Zr molar ratio
SiZr5-1.5Ni	856.3	874.1	0.12	0.11
SiZr5-3Ni	856.3	874.2	0.27	0.23
SiZr5-6Ni	854.5 (58%)	872.4	0.32	0.47
	856.6 (42%)	874.5		
SiZr5-12Ni	854.5 (66%)	872.3	0.840	1.02
	856.6 (34%)	874.9		

which makes the detection by XPS of nickel atoms inside these large particles difficult, giving rise to a lower atomic concentration of surface nickel in comparison with that deduced from the bulk analysis.

The Ni 2p core level signal of the studied catalysts is different depending on the nickel concentration. For the catalysts with low nickel content, the Ni $2p_{3/2}$ signal is symmetric and sharp, with a maximum centred at 856.3 eV (Fig. 2), associated with the Ni $2p_{1/2}$ doublet at 874.2 eV. The binding energy of the Ni $2p_{3/2}$ peak is shifted around 2.0 eV to higher values compared to that of NiO (854.2 eV),[20] and can be assigned to NiO present as small particles inside the mesopores. However, the Ni 2p XPS spectra of the catalysts with high nickel content (Fig. 2) show a broad and asymmetric Ni $2p_{3/2}$ signal which can be deconvoluted in two peaks at 854.5 and 856.6 eV (Table 2). The more intense peak (at 854.5 eV) is assigned to octahedral Ni^{2+} forming part of the large particles of NiO deposited on the external surface of the mesoporous support. This binding energy value is close to that observed for unsupported NiO (854.2 eV).[20] The second, less intense peak appears at 856.6 eV, very near to those arising from the SiZr5-1.5Ni and SiZr5-3Ni catalysts, and, as previously pointed out, corresponds to small nickel oxide particles. Therefore, the XRD and XPS data support the existence of a bimodal particle size distribution, with small and large nickel oxide particles, as observed by Meng *et al.*[10] in the case of NiO supported on MCM-41, with 10 wt% Ni.

This family of catalysts was also studied by H_2-TPR (Fig. 3). Bulk nickel oxide is reduced between 300 and 400 °C,[21,22] thus, the H_2-TPR of bulk NiO, prepared from $Ni(NO_3)_2$ by calcination, shows a single broad H_2 consumption signal centred at 350 °C.[11] Furthermore, NiO supported on silica is reduced at 400–500 °C,[21,22] and in some cases, temperatures higher than 600 °C have been reported.[22] According Takahashi *et al.*,[22] the calcination conditions affect not only the particle size, but also the reducibility of the NiO species. The H_2-TPR profile for the sample with the lowest nickel content (SiZr5-1.5Ni) shows a

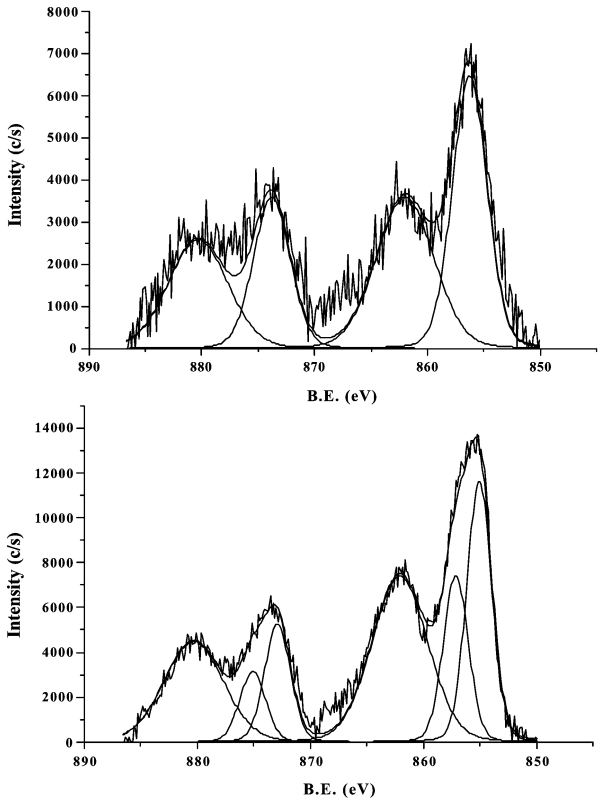

Fig. 2 Ni 2p core level spectra for SiZr5-3Ni (A) and SiZr5-12Ni (B) catalysts.

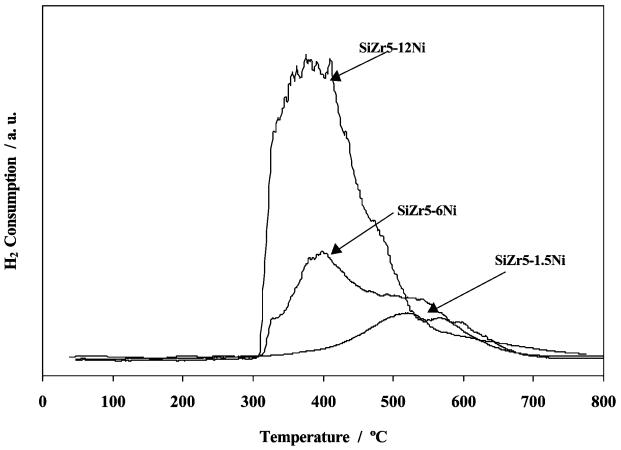

Fig. 3 H_2-TPR curves of the supported nickel oxide catalysts.

broad H_2 consumption band with maxima at high temperatures, between 530 and 600 °C. As expected, the reduction of Ni^{2+} inside the mesopores is more difficult because of the strong interaction between the metallic ion and the support, as suggested by the high binding energy value of the Ni $2p_{3/2}$ photoemission. On the other hand, the H_2-TPR profile for the sample with the highest nickel content (SiZr5-12Ni) exhibits a single and very broad reduction signal between 300 and 400 °C, and a shoulder at 490 °C. The temperature of the maximum is the same than that observed for isolated NiO, whereas the shoulder at higher temperature may correspond to the reduction of Ni(II) inside the mesopores. Moreover, a relationship between the reduction temperature and the binding energy of the Ni $2p_{3/2}$ photoemission can be established, since a low Ni $2p_{3/2}$ binding energy (854.5 eV) is associated with a low reduction temperature. The H_2-TPR profile of the SiZr5-6Ni catalyst is intermediate between the two profiles described above. There is a maximum centred at 390 °C, which can be attributed to the reduction of large NiO particles, and a broad shoulder between 480 and 540 °C due to the reduction of Ni(II) inside the mesopores.

The total acidity values of the catalysts, determined by NH_3-TPD, are shown in Table 1. The acidity increases for the catalysts with lower nickel contents because Ni^{2+} has a tendency to form amino complexes. However, with higher nickel loadings, large NiO particles formed on the surface could partially block the access of ammonia to acidic centres. Thus, the catalyst with the highest nickel loading (SiZr5-12Ni) exhibits the lowest total acidity.

The NO-TPD curves of the studied catalysts are shown in Fig. 4. Two types of desorption curves are again observed. The SiZr5-1.5Ni and SiZr5-3Ni catalysts present NO very similar

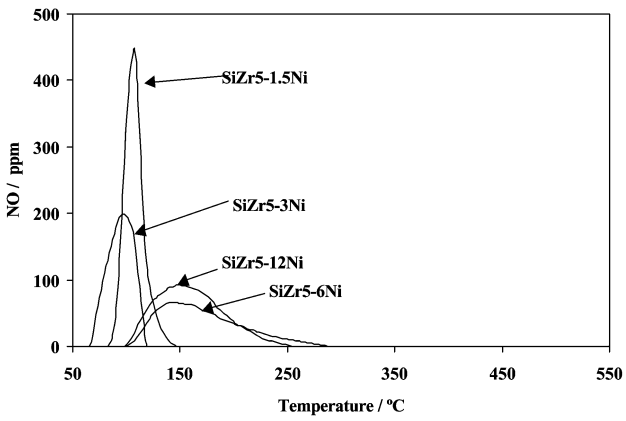

Fig. 4 TPD curves for NO on supported nickel oxide catalysts.

desorption curves, with a single peak centred at a temperature as low as 100 °C. This desorption peak may correspond to NO molecules weakly interacting with small NiO particles, which interact strongly with the support. However, the catalysts with high nickel loading present broad desorption curves between 100–250 °C, with maxima centred at about 150 °C, but with much lower intensity than those observed for the low nickel loading catalysts. This high desorption temperature suggests that NO molecules interact more strongly with large NiO particles.

Catalytic activity

This family of new catalysts has been tested in the SCR of NO with ammonia in the presence of excess oxygen, according to reaction 1.

$$4\ NH_3 + 4\ NO + O_2 \rightarrow 4\ N_2 + 6\ H_2O \qquad (1)$$

The NO reduction curves as a function of the reaction temperature for the different nickel catalysts (at a space velocity of 3300 h^{-1}) are shown in Fig. 5. These curves reflect the fact that the nickel loading not only influences the NO conversion but, more especially, the temperature of maximum NO conversion. Thus, the catalyst with the lowest nickel content (SiZr5-1.5Ni) exhibits the lowest catalytic activity, with a maximum NO conversion (*ca.* 25%) attained at high temperature (500 °C). However, the catalyst with a nickel loading of 3 wt% presents a much higher catalytic activity (53% of NO conversion), but at a similar reaction temperature. It is very interesting to note that the working temperature range is shifted to lower values as the nickel loading increases. The maximum conversion was reached with the SiZr5-6Ni catalyst, which presents a value close to 60%. These results are in contrast with those reported for cobalt oxide and copper oxide impregnated on the same support,[6,7] where NO conversion values higher than 85% at lower temperatures (200–300 °C) were attained. On the other hand, the catalytic activity data are in agreement with the reducibility of supported nickel oxide. This reducibility was previously evaluated by H_2-TPR, confirming that Ni(II) species are more easily reduced in the case of high nickel loading catalysts, which are, in turn, the catalysts which give maximum NO conversion. Although, there are no data about the role of Ni^{2+} in the scarce literature regarding the use of nickel oxide as the active phase in the NO SCR, these results seem to indicate that the reduction of Ni^{2+} to Ni^{+} could be participating in the mechanism governing this reaction, similarly to the situation with copper oxide.[23] This assumption is supported by the findings of Hartmann *et al.*[24] concerning the existence of Ni^{+} when Ni^{2+} is ion-exchanged in a similar support, aluminium-doped mesoporous silica.

It is interesting to note that even at 400 °C, where the maximum NO conversion is attained, the formation of N_2O according to reaction 2 is minimal, being only 61 ppm for the most active catalyst (SiZr5-6Ni) and negligible for the least active catalyst (SiZr5-1.5Ni) (see Fig. 6). However, N_2O can also be formed from ammonia oxidation (reaction 3).

$$4\ NH_3 + 4\ NO + 3\ O_2 \rightarrow 4\ N_2O + 6\ H_2O \qquad (2)$$

$$2\ NH_3 + 2\ O_2 \rightarrow N_2O + 3\ H_2O \qquad (3)$$

In Fig. 7, the selectivity in the NO SCR as a function of the reaction temperature is shown, this selectivity being defined as

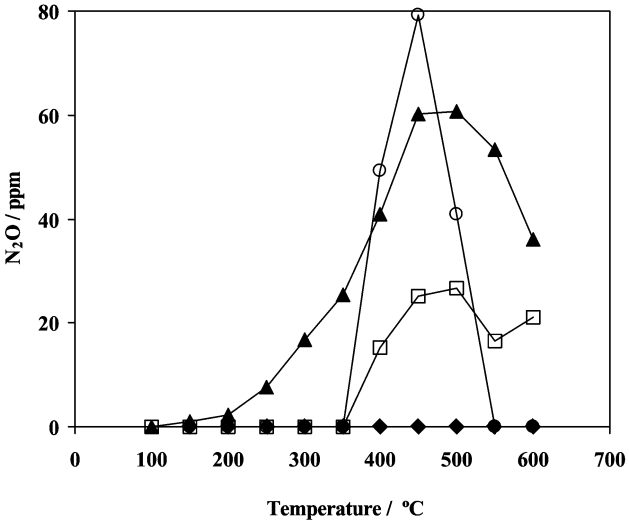

Fig. 6 Formation of N_2O as a function of the reaction temperature for SiZr5-1.5Ni (◆), SiZr5-3Ni (□), SiZr5-6Ni (▲) and SiZr5-12Ni (○) catalysts.

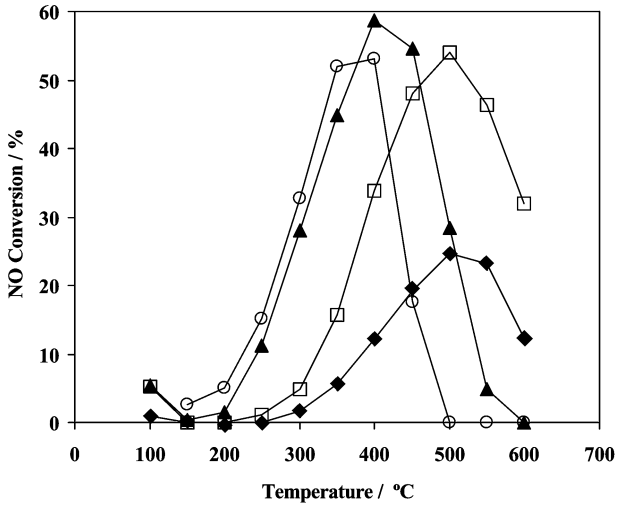

Fig. 5 NO conversion as a function of the reaction temperature for (a) SiZr5-1.5Ni (◆), SiZr5-3Ni (□), SiZr5-6Ni (▲) and SiZr5-12Ni (○) catalysts.

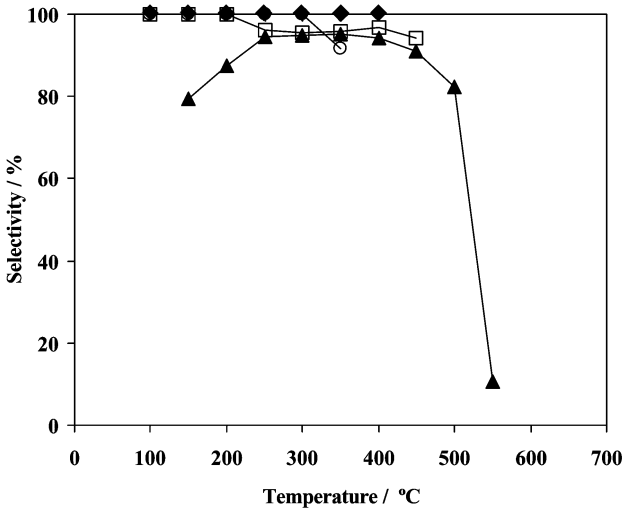

Fig. 7 Variation of selectivity (%) in the SCR reaction, defined as in eqn. 4, as a function of the reaction temperature for SiZr5-1.5Ni (◆), SiZr5-3Ni (□), SiZr5-6Ni (▲) and SiZr5-12Ni (○) catalysts.

Table 3 Catalytic data for the SCR of NO at 400 °C

Sample	NO conversion (%)	NH_3 conversion (%)	N_2 (ppm)	N_2O (ppm)	Selectivity (%)	Yield (%)	Activity/μmol NO g^{-1} s^{-1}	TOF × 10^4/molecule NO s^{-1} at_{Ni}^{-1}
SiZr5-1.5Ni	12.1	42.9	296	0	100	12	0.026	5.5
SiZr5-3Ni	33.9	47.0	452	15	96	32	0.075	16.0
SiZr5-6Ni	58.7	66.7	690	41	94	55	0.137	29.0
SiZr5-12Ni	53.0	96.7	764	49	92	49	0.114	24.0

$$\text{Selectivity (\%)} = 100 \times ([NO]_{red} - [N_2O])/[NO]_{red} \quad (4)$$

where $[NO]_{red}$ is the difference between $[NO]_{initial}$ and $[NO]_{final}$. At 400 °C, the selectivity is very high, close to 92% for all the catalysts, although the yield of N_2 is at a maximum for SiZr5-12Ni (see Table 3). At higher temperatures, the selectivity decreases for the most active catalyst, which could be due to secondary reactions favoured at these temperatures.

As regards the NH_3 conversion as a function of the reaction temperature (Fig. 8), it can be seen that although from 400 °C the NO conversion decreases, the NH_3 conversion continues increasing for all the catalysts except SiZr5-12Ni. This fact can be attributed to the formation of N_2 and N_2O (Fig. 6 and 9) by non-selective NH_3 oxidation processes (reactions 3 and 5).

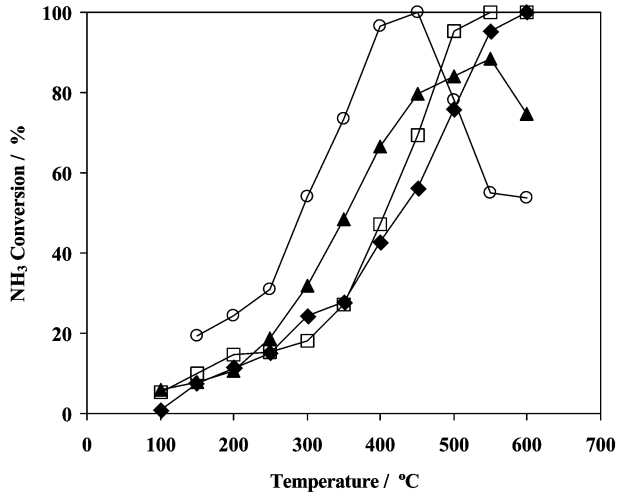

Fig. 8 NH_3 conversion as a function of the reaction temperature for SiZr5-1.5Ni (◆), SiZr5-3Ni (□), SiZr5-6Ni (▲) and SiZr5-12Ni (○) catalysts.

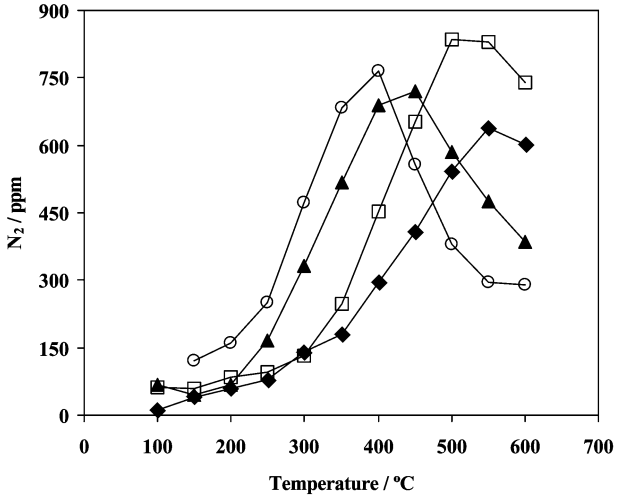

Fig. 9 Formation of N_2 as a function of the reaction temperature for SiZr5-1.5Ni (◆), SiZr5-3Ni (□), SiZr5-6Ni (▲) and SiZr5-12Ni (○) catalysts.

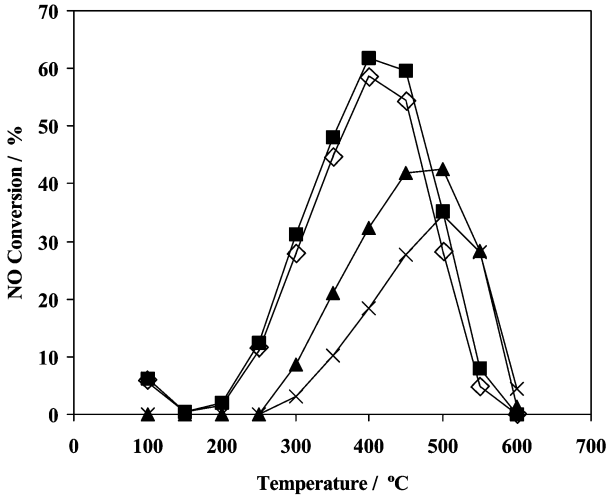

Fig. 10 NO conversion as a function of the reaction temperature on the supported nickel oxide catalysts at different space velocities (h^{-1}): 2146 (■), 3300 (◊), 7500 (▲), 12012 (×) h^{-1}.

$$2\ NH_3 + 3/2\ O_2 \rightarrow N_2 + 3\ H_2O \quad (5)$$

The influence of the space velocity on the NO conversion was studied by varying this parameter from 2000 to 12 000 h^{-1} and using the most active catalyst, SiZr5-6Ni. Fig. 10 shows that the NO conversion is affected for space velocities higher than 3300 h^{-1}, leading to a decrease in the NO conversion and a shift of the temperature of maximum conversion at higher values. However, the amount of N_2O formed is not affected by the decrease in the residence time of reactants on the catalyst, the maximum N_2O production only being shifted at higher temperatures with an increase in the space velocity. The NH_3 conversion increases with the reaction temperature for all the studied space velocities, this fact and the decrease of the NO conversion at high temperatures indicate that N_2 and N_2O mainly come from the non-selective oxidation of NH_3.

The effect of the partial pressure of O_2 on the NO SCR has also been studied by varying the amount of O_2 in the feed between 0.25 and 3.5 vol%. As the partial pressure of O_2 was raised up to 2.5 vol%, the NO conversion increased and, concomitantly, the temperature of maximum conversion shifted to lower values. The formation of N_2O and N_2 is favoured by increasing the partial pressure of O_2, attaining a maximum value for at $P(O_2) = 2.5$ vol%. The NH_3 conversion increases with $P(O_2)$ and an NH_3 conversion of 100% is observed with a feed of 3.5 vol% O_2, indicating the participation of the non-selective oxidation of ammonia in N_2O and N_2 formation.

The SCR of NO also depends on the partial pressure of NH_3. The NO conversion increases with the concentration of NH_3 up to a maximum value of 63% at 450 °C and 1500 ppm NH_3. However, at higher partial pressures of NH_3, a decrease in the NO conversion and an increase in N_2O and N_2 formation were observed. Finally, the SCR of NO with NH_3 strongly depends

on the concentration of NO in the feed, since the NO conversion dramatically decreases and the maximum conversion is shifted at higher temperatures when NO concentrations higher than 1000 ppm are employed.

The SiZr5-6Ni catalyst is very stable under the experimental conditions tested, its activity being maintained after 8 h of time-on-stream. Although its catalytic activity become zero at 600 °C, its maximum activity is completely recovered when the catalytic reaction is again carried out at 400 °C.

For this catalyst, we can conclude that nickel oxide supported on a zirconium-doped mesoporous silica is active as a catalyst for NO SCR, and the catalytic activity can be related to both the high NiO dispersion and the size of the NiO crystallites.[10] The crystallites of NiO in SiZr5-6Ni are mainly located on the external surface, interacting weakly with the support and being accessible and easily reducible for active participation in the SCR of NO. However, a nickel content of 12 wt% lowers the catalytic activity because the lesser degree of dispersion of the active phase and to its greater tendency to oxidise NH_3 directly to N_2O.

Acknowledgement

This research was performed under the Contract No. BRPR CT97 0545 of the European Union.

References

1 R. J. Farrauto, R. M. Heck and B. K. Speronello, *Chem. Eng. News*, 1992, September 7, 34.
2 A. Baiker, M. A. Reiche and D. C. M. Dutoit, *Appl. Catal., B*, 1997, **13**, 275.
3 G. Busca, L. Lietti, G. Ramis and F. Berti, *Appl. Catal., B*, 1998, **18**, 1.
4 Y. Traa, B. Burger and J. Weitkamp, *Microporous Mesoporous Mater.*, 1999, **30**, 3.
5 A. Z. Ma, M. Muhler and W. Grünert, *Appl. Catal., B*, 2000, **27**, 37.
6 R. Moreno-Tost, J. Santamaría-González, P. Maireles-Torres, E. Rodríguez-Castellón and A. Jiménez-López, *Appl. Catal., B*, 2002, **38**, 51.
7 R. Moreno-Tost, P. Braos-García, J. Santamaría-González, P. Maireles-Torres, E. Rodríguez-Castellón and A. Jiménez-López, *Catal. Lett.*, 2002, in press.
8 J. S. Beck, J. C. Vartuli, W. J. Roth, M. E. Leonowicz, C. T. Kresge, K. D. Schmitt, C. T. W. Chu, D. H. Olsen, E. W. Sheppard, S. B. McCullen, J. B. Higgins and J. L. Schlenker, *J. Am. Chem. Soc.*, 1992, **114**, 10834.
9 R. T. Yang, T. J. Pinnavaia, W. Li and W. Zhang, *J. Catal.*, 1997, **172**, 488.
10 M. Meng, P. Lin and Y. Fu, *Spectrosc. Lett.*, 2001, **34**, 83.
11 D. J. Lensveld, J. G. Mesu, A. J. van Dillen and K. P. de Jong, *Microporous Mesoporous Mater.*, 2001, **44–45**, 401.
12 A. Corma, A. Martínez, V. Martínez-Soria and J. B. Montón, *J. Catal.*, 1995, **153**, 25.
13 T. Halachev, R. Nava and L. Dimitrov, *Appl. Catal., A.*, 1998, **169**, 111.
14 T. Klimova, J. Ramírez, M. Calderón and J. M. Domínguez, *Stud. Surf. Sci. Catal.*, 1998, **117**, 493.
15 M. Ziolek, I. Nowak, I. Sobcsak and H. Poltorak, *Stud. Surf. Sci. Catal.*, 2000, **130**, 3047.
16 D. J. Jones, J. Jiménez-Jiménez, A. Jiménez-López, P. Maireles-Torres, P. Olivera-Pastor, E. Rodríguez-Castellón and J. Rozière, *Chem. Commun.*, 1997, 431.
17 A. Jiménez-López, E. Rodríguez-Castellón, P. Maireles-Torres, L. Díaz and J. Mérida-Robles, *Appl. Catal., A.*, 2001, **218**, 295.
18 R. Hernández-Huesca, J. Mérida-Robles, P. Maireles-Torres, E. Rodríguez-Castellón and A. Jiménez-López, *J. Catal.*, 2001, **203**, 122.
19 A. B. P. Lever, *Inorganic Electronic Spectroscopy*, Elsevier, Amsterdam, 1988.
20 J. C. Klein and D. M. Hercules, *J. Catal.*, 1983, **82**, 424.
21 B. Mile, D. Stirling, M. A. Zammitt, A. Lowell and M. Webb, *J. Catal.*, 1998, **114**, 217.
22 R. Takahashi, S. Sato, T. Sodesawa, M. Kato, S. Takenata and S. Yoshida, *J. Catal.*, 2001, **204**, 259.
23 G. Ramis, Y. Li, G. Busca, M. Turco, E. Kortur and R. J. Willey, *J. Catal.*, 1995, **157**, 523.
24 M. Hartmann, A. Pöppl and L. Kevan, *J. Phys. Chem.*, 1996, **100**, 9906.